Excitons in Chains of Dimers

Vladas Liuolia,[†] Leonas Valkunas,[*,†] and Rienk van Grondelle[‡]

Institute of Physics, A. Gostauto 12, 2600 Vilnius, Lithuania, and Department of Biophysics, Faculty of Physics and Astronomy, Vrije Universiteit Amsterdam, de Boelelaan 1081, 1081 HV Amsterdam, The Netherlands

Received: December 3, 1996; In Final Form: May 1, 1997[⊗]

Excitons in circular aggregates of dimers are discussed with the aim to understand the possible spectral and energy transfer properties of the ringlike peripheral complexes of photosynthetic bacteria. The system is explicitly heterogeneous (i.e., the difference in transition energies of the molecules within the dimer as, well as the difference in the intra- and interdimer resonance interactions, is accounted for). It is demonstrated that the energy spectrum of such a system exhibits many of the features as observed in spectrally inhomogeneous circular aggregates. The model is used to illustrate the changes in absorption and circular dichroism spectra that take place upon incorporating a dimer into a circular chain. The exciton dynamics in the aggregate is considered in the Haken−Strobl−Reineker approach. When terms are neglected describing the phase relaxation between nonnearest neighbors, the equations for the diagonal density matrix elements are obtained containing both coherent exciton motion within the dimer—the building block of the aggregate—and an incoherent hopping of the excitation between dimers. It is demonstrated that these equations contain a wavelike soliton solution (if dephasing is absent) as well as a diffusion-like solution (for large dephasing rates).

Introduction

The initial event in photosynthesis is the absorption of light by the light-harvesting antenna (LHA), which is followed by a rapid and efficient transfer of the absorbed energy to the reaction center (RC), where charge separation is initiated.[1] The crystal structures of the peripheral light-harvesting antenna complexes (LH2) of the photosynthetic bacteria *Rhodopseudomonas (Rps.) acidophila*[2,3] and *Rhodospirillum (Rh.) molischianum*[4] have shown their ringlike organization. A similar ringlike structure is also present in the core light-harvesting complex LH1.[5] Both these structures elegantly demonstrate how in such a ring a bacteriochlorophyll (Bchl) oligomer is organized using two spatial scaling parameters. The presence of two nonequivalent binding sites for adjacent pigment molecules in the aggregate, dictated by the two proteins involved, introduces two characteristic distances and orientational factors.

So far, the theoretical consideration of ringlike molecular aggregates has been concentrated on the analysis of aggregates with one scaling parameters, or in other words, on aggregates with only one molecule per unit cell.[6,7] On the other hand, a numerical analysis of the spectral properties of the ringlike molecular aggregate was also carried out[8] by using the X-ray structural data of the *Rp. acidophila* LH2. In addition, the spectral inhomogeneity of the molecules in the aggregate has been considered.[9] However, the presence of two scaling parameters in the system (aggregates with two molecules per unit cell) provides additional degrees of freedom in modeling absorption and circular dichroism (CD) spectra. Similarly, the excitation transfer dynamics will depend on the two scaling parameters, a fact that until now has not been explicitly considered.[22] Thus, the aim of this work is to describe the spectroscopy and excitation dynamics in these ringlike molecular aggregates with two molecules per unit cell and to discuss the applicability of this approach for bacterial light-harvesting complexes LH2/1. It is worth mentioning that this model, in

which we assume that the two molecules in the unit cell are characterized by different transition energies, already exhibits the basic features of spectrally inhomogeneous systems, while all the results can be obtained analytically. In our modeling two limiting cases can be distinguished. In the first case, for which the intermolecular distance within the unit cell is much smaller than the distance between molecules from a neighboring unit cells, we have the system of weakly interacting asymmetric dimers. In the second case, the difference between the transition energies of the molecules within the same unit cell dominates, corresponding to an extremely large value for the Davydov splitting.[10]

Exciton Spectrum

The spectrum of a molecular aggregate is determined by solving the stationary Schrödinger equation. Due to the weak intermolecular interactions, the Heitler−London approximation can be used,[10] which means that these weak intermolecular interactions can be considered as a perturbation of the energy spectrum, while the eigenfunctions of the aggregate in first order are given by linear combinations of the product of the molecular eigenfunctions. At first let us neglect the interaction of the electronic excitation with intermolecular vibrations/phonons, by assuming that all molecules have fixed positions. The Hamiltonian H of the molecular aggregate in this approximation is then as follows[10]:

$$H = \sum_{n_\alpha} \Delta_{n_\alpha} b_{n_\alpha}{}^\dagger b_{n_\alpha} + \sum_{n_\alpha \neq m_\beta} V_{n_\alpha,m_\beta} b_{n_\alpha}{}^\dagger b_{m_\alpha} \qquad (1)$$

where n and m run over the N unit cells in the aggregate and α and β enumerate the position of the molecule within the unit cell. Δ_{n_α} is the site energy of the nth molecule and V_{n_α,m_β} is the interaction (transfer integral) between molecules $n\alpha$ and $m\beta$, $b^\dagger_{n_\alpha}$, b_{n_α} are creation, annihilation operators for excitation of the corresponding molecule. The eigenfunctions of a separate excited molecule n_α are described by

$$|n_\alpha\rangle = b_{n_\alpha}{}^\dagger |0\rangle \qquad (2)$$

* Corresponding author.
† Institute of Physics.
‡ Vrije Universiteit Amsterdam.
⊗ Abstract published in *Advance ACS Abstracts,* August 15, 1997.

Figure 1. Schematic representation of the dimerized molecular aggregate characterized by two scaling intermolecular distances: *a* and *b*.

where $|0\rangle$ is the eigenfunction of the aggregate ground state. Due to translation symmetry according to the Bloch theorem we have $V_{n_\alpha, m_\beta} = V_{\alpha\beta}(n - m)$.

The *H*amiltonian *H* can easily be diagonalized by a transformation to the quasi momentum representation with the new set of creation and annihilation operators

$$a^\dagger_{kv} = \frac{1}{\sqrt{N}}\sum_{n_\alpha} u^*_{\alpha v}b^\dagger_{n_\alpha} \exp(-ikn_\alpha)$$

$$a_{kv} = \frac{1}{\sqrt{N}}\sum_{n_\alpha} u_{\alpha v}b_{n_\alpha} \exp(ikn_\alpha) \qquad (3)$$

where *k* is the wave vector $k = \frac{2\pi}{N}j, -\frac{N}{2} < j \leq \frac{N}{2}$ and v accounts for the splitting of degenerate molecular states into σ molecular subbands (σ is the number of molecules per unit cell). Substituting eqs 3 into the Schrödinger equation leads to a set of σ equations for the elements of the matrix *u(k)*

$$\sum_\beta L_{\alpha\beta}(k)u_{\beta v}(k) = E_v(k)u_{\alpha v}(k) \qquad (4)$$

where

$$L_{\alpha\beta}(k) = \sum_{n-m}\{\Delta_\alpha\delta_{\alpha\beta} + V_{\alpha\beta}(n - m)e^{-ik(n_\alpha - m_\beta)}\} \qquad (5)$$

Since the transformation coefficients are normalized, we have

$$\sum_\alpha |u_{\alpha v}(k)|^2 = 1 \qquad (6)$$

Thus, the excited state spectra are determined via the corresponding characteristic equation

$$det\{L_{\alpha\beta}(k) - E_v(k)\} = 0 \qquad (7)$$

Matrix 5 is Hermitian, thus all σ values of $E_v(k)$ are real. These $E_v(k)$ determine σ exciton subbands and this phenomenon is known as Davydov splitting.

Let us now consider a linear (cyclic) molecular aggregate with two molecules per unit cell assuming that the distance parameter *b* determines the intermolecular distance within the unit cell and *a* is the intermolecular scaling parameter between the neighboring cells (see Figure 1). The diagonalizaton procedure 3 now yields the following analytical solution for the energies $E_v(k)$:

$$E_v(k) = \frac{\Delta_1 + \Delta_2}{2} - (-1)^v\sqrt{\left(\frac{\Delta_1 - \Delta_2}{2}\right)^2 + |L_{12}(k)|^2} \qquad (8)$$

In the case of the "nearest neighbor" approximation, in which only interactions between neighboring chromophores are considered, we have

$$L_{12}(k) = V_a e^{-ika} + V_b e^{ikb} \qquad (9)$$

$$|L_{12}(k)|^2 = V_a^2 + V_b^2 + 2V_a V_b \cos k(a + b)$$

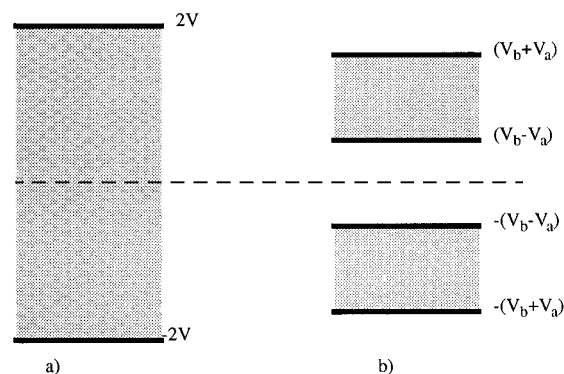where $V_{a,b}$ determine the corresponding matrix elements for

Figure 2. Exciton bands for an aggregate with a single molecule per unit cell (a) and for a homogeneous aggregate with two molecules per unit cell (b). The black lines show the edges of the bands; the unperturbed energy is represented by the dashed line in the center of the band.
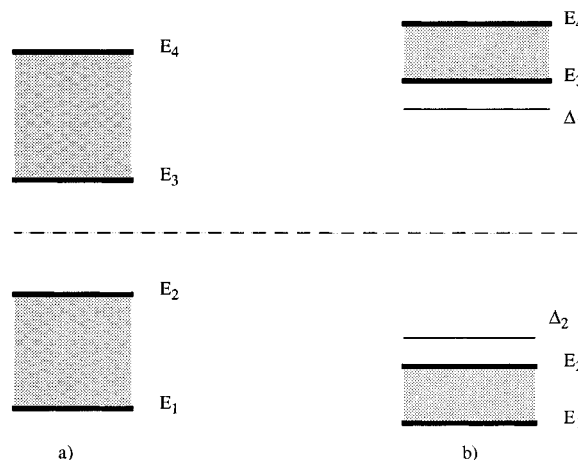

Figure 3. Exciton subbands for molecular aggregates with two heterogeneous molecules per unit cell. The black lines show the edges of the bands; the unperturbed energy is represented by the dashed line in the center of the band. (a) corresponds to the case of equal resonance interactions, thus, $E_4 - E_1 = 2[((\Delta_1 - \Delta_2)/2)^2 + 4V_a^2]^{1/2}$ while b) corresponds to the case of large heterogeneity in unit cell, or $E_4 - E_1 = \Delta_1 - \Delta_2 + 2(V_b + V_a)^2/(\Delta_1 - \Delta_2)$ and $E_3 - E_2 = \Delta_1 - \Delta_2 + 2(V_b - V_a)^2/(\Delta_1 - \Delta_2)$.

resonance interactions. A variation in the value of the molecular site displacement energy, measured by $\Delta_1 - \Delta_2$ and inherent to our definition of the unit cell, is responsible for the heterogeneous broadening of the spectra.

Furthermore, in such a dimerized aggregate the different value of the two spatial scaling parameters *b* and *a* (with *b* < *a*) is taken to be responsible for the difference in resonance interaction ($V_b > V_a$). Alternatively, the value of the orientation parameter may vary. For such a chain of dimers eq 8 then immediately leads to a splitting of the exciton band into two Davydov subbands, which are separated by $2(V_b - V_a)$, even in the absence of heterogeneity of the two molecules in the unit cell (i.e., for $\Delta_1 = \Delta_2$). The dimerization also leads to a narrowing of the exciton band, i.e. the bandwidth changes from $4V_b$ for the aggregate with a single molecule per unit cell to $2(V_b - V_a)$ for the chain of dimers (see Figure 2). Introducing heterogeneity for the unit cell ($\Delta_1 \neq \Delta_2$) changes the total bandwidth, which becomes equal to $2[((\Delta_1 - \Delta_2)/2)^2 + (V_b + V_a)^2]^{1/2}$ and increases the size of the energy gap between the $V_b + V_a$ Davydov subbands to $2[((\Delta_1 - \Delta_2)/2)^2 + (V_b - V_a)^2]^{1/2}$. Thus, even for equal intermolecular distances and equivalent orientations (i.e. at $V_a = V_b$) the exciton band is also disturbed. In that case the exciton bandwidth is $2[((\Delta_1 - \Delta_2)/2)^2 + 4V_a^2]^{1/2}$ and the gap in the energy level diagram, which separates the Davydov subbands, equals $|\Delta_1 - \Delta_2|$ (see Figure 3).

Excitons in Chains of Dimers

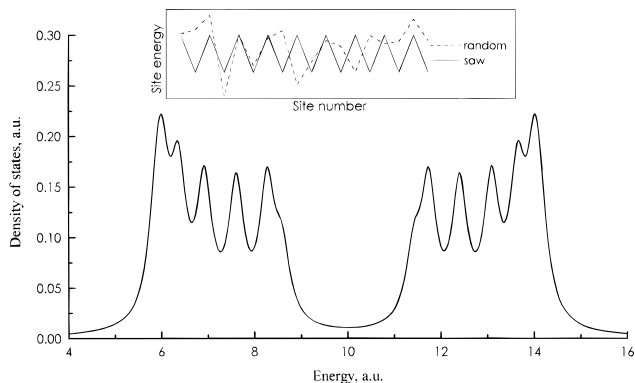*J. Phys. Chem. B, Vol. 101, No. 37, 1997* **7345**

Figure 4. Density of states for the dimerized chain with heterogeneous unit cells and taking $N = 9$. In the inset we show for illustration, the energy surface corresponding to a heterogeneous unit cell (solid line) together with one of the realizations of a random distribution (dashed line).

We note that in the limiting case of a very large intermolecular distance between the cells (i.e., when $a \gg b$ (or $V_a \approx 0$) eq 8 gives the well-known result for the energy spectrum of the dimer with inequivalent site energies. Thus, we conclude that a difference in the resonance interaction between molecules within a unit cell and between the molecules from different unit cells alters the exciton bandwidth and creates a gap between the Davydov subbands in the center of the total exciton band. A very similar effect can be obtained by assuming the molecules in the unit cell to be energetically heterogeneous. The spectral density of states $\rho(\epsilon)$ for an aggregate with mutually parallel dipole moments and cyclic boundary conditions reads[11]

$$\rho(\epsilon) = -\frac{1}{\pi} Im \left(\frac{1}{N\sigma} \sum_{k,\nu} \frac{1}{\epsilon - E_\nu(k) + i\delta} \right) \quad (10)$$

where ImA means the imaginary part of A, δ is the homogeneous line width. The spectral density of states for the dimerized aggregate seems to be the simplest model that contains some of the basic features manifested by disordered systems. This originates from the "sawlike" site energy distribution, created by the heterogeneity of the molecules within a unit cell. The similarity is clearly seen by comparing the results presented in Figure 4 with the Monte-Carlo simulations for an aggregate with diagonal disorder.[9]

The strength of the optical transition to the exciton state is given by the corresponding dipole strength:

$$A_\nu(k) = \frac{1}{N} \sum_{\alpha, \beta} u_{\alpha\nu}(k) u^*_{\beta\nu}(k) \sum_{n,m} e^{ik(n_\alpha - m_\beta)} (\vec{d}_{n_\alpha} \cdot \vec{d}_{m_\beta}) \quad (11)$$

where $\vec{d}_{n_\alpha} = \langle 0|\vec{d}|n\alpha \rangle$ is the transition dipole moment and $\vec{d}$ is the corresponding dipole moment operator.

Let us now consider the case of a cyclic molecular aggregate with two molecules per unit cell, the exciton spectrum of which is defined in eq 8. Similar to the cyclic aggregate with a single molecule per unit cell, the relative orientations of the transition dipole moments and their dependence on the position in the aggregate are important. In the notation of Figure 5, the scalar product of transition dipole moments is described as follows:

$$\vec{d}_{n_\alpha} \cdot \vec{d}_{m_\beta} = d^2 \{ \sin \theta_\alpha \sin \theta_\beta \cos[\gamma(n - m) + \gamma'(\alpha - \beta) + \varphi_\alpha - \varphi_\beta] + \cos \theta_\alpha \cos \theta_\beta \} \quad (12)$$

where α and β determine the position of the molecules in the unit cells (i.e., being equal to 1 and 2 according to the definitions of Figure 5), γ and γ' are the turning angles between the
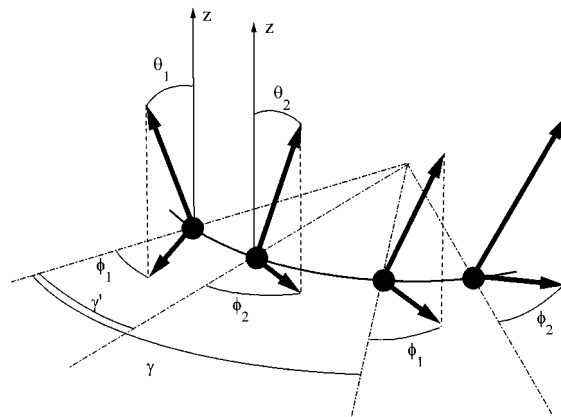

Figure 5. Model structure of the circular dimerized aggregate.

transition dipole moments of the neighboring molecules from different unit cells and within the same cell, respectively (i.e., $\gamma = \frac{2\pi}{N}$, $0 \leq \gamma' \leq \gamma$), and d is the absolute value of the molecular transition dipole moment.

Due to the fact that in aggregates with periodic boundary conditions we can change the sum over n by the sum over $n - m$, only transitions into six exciton states are not equal to zero, with two pairs of states (see also ref 8):

$$A_\nu(\pm\gamma) = \frac{1}{2} Nd^2 \sum_{\alpha, \beta} u_{\alpha\nu}(\pm\gamma) u^*_{\beta\nu}(\pm\gamma) \times$$
$$\sin \theta_\alpha \sin \theta_\beta e^{\pm i(\gamma'(\alpha - \beta) + \varphi_\alpha - \varphi_\beta)} \quad (13)$$

for the degenerate states of the aggregate and

$$A_\nu(0) = Nd^2 \sum_{\alpha, \beta} u_{\alpha\nu}(0) u^*_{\beta\nu}(0) \cos \theta_\alpha \cos \theta_\beta \quad (14)$$

for the nondegenerate states.

To determine the coefficients $u_{\alpha\nu}(k)$, we will use the corresponding set of eqs 4 as well as the values of the exciton energies determined by eq 8. By taking into account the normalization conditions as given by eq 6, the following relations are derived:

$$|u_{1\nu}(k)|^2 \equiv |u_{1\nu}(-k)|^2 =$$
$$\frac{|L_{12}(k)|^2}{|L_{12}(k)|^2 + (E_\nu(k) - \Delta_1)^2} = \frac{F_\nu(k)^2}{F_\nu(k)^2 + 1}$$

$$|u_{2\nu}(k)|^2 \equiv |u_{2\nu}(-k)|^2 =$$
$$\frac{(E_\nu(k) - \Delta_1)^2}{|L_{12}(k)|^2 + (E_\nu(k) - \Delta_1)^2} = \frac{1}{F_\nu(k)^2 + 1} \quad (15)$$

where $F_\nu(k) = \frac{|L_{12}(k)|}{E_\nu(k) - \Delta_1}$, and

$$u_{1\nu}(k) u^*_{2\nu}(k) = \frac{L_{12}(k)}{E_\nu(k) - \Delta_1} |u_{2\nu}(k)|^2 \quad (16)$$

Correspondingly, by substituting these expressions into eqs 13 and 14, we obtain:

$$A_\nu(\gamma) + A_\nu(-\gamma) = \frac{Nd^2}{F_\nu(\gamma)^2 + 1} \left\{ F_\nu(\gamma)^2 \sin \theta_1^2 + \sin \theta_2^2 + 2F_\nu(\gamma) \frac{ReL_{12}(\gamma)}{|L_{12}(\gamma)|} \cos(\varphi_1 - \varphi_2) \sin \theta_1 \sin \theta_2 \right\} \quad (17)$$

and

$$A_\nu(0) = \frac{Nd^2}{F_\nu(0)^2 + 1}[F_\nu(0)\cos\theta_1 + \cos\theta_2]^2 \quad (18)$$

where in our notations, with $k(a + b) = \gamma j$ and $kb = \gamma' j$, we have:

$$ReL_{12}(k) = V_a\cos[j(\gamma' - \gamma)] + V_b\cos j\gamma \quad (19)$$

Equations 17 and 18 show that we have two allowed transitions into each Davydov subband. However, in case all transition moments are within the plane of the aggregate (i.e., when $\theta_1 = \theta_2 = \frac{\pi}{2}$), the dipole strength into the states $k = 0$ vanishes and only the transitions into the states $k = \pm\gamma$ remain for each subband.

From the orientations and distances we furthermore can calculate the CD spectrum, which in general is given by:[12,13]

$$C_\nu(k) \sim \frac{1}{N}\sum_{\alpha,\beta}u_{\alpha\nu}(k)u^*_{\beta\nu}(k)\sum_{n,m}e^{ik(n_\alpha - m_\beta)}[\vec{r}_{n_\alpha n_\beta}\cdot\vec{r}_{n_\alpha}\times\vec{r}_{m_\beta}] \quad (20)$$

The CD amplitude for a dimerized chain is proportional to

$$C_\nu(0) \sim \frac{rNd^2}{F_\nu(0)^2 + 1}(F_\nu(0)^2\sin 2\theta_1\sin\varphi_1 + \sin 2\theta_2\sin\varphi_2 +$$

$$2F_\nu(0)H(0)) \quad (21)$$

$$C_\nu(\gamma) \sim \frac{-rNd^2}{F_\nu(\gamma)^2 + 1}(F_\nu(\gamma)^2\sin 2\theta_1\sin\varphi_1 +$$

$$\sin 2\theta_2\sin\varphi_2 + 2F_\nu(\gamma)H(\gamma)) \quad (22)$$

where r is the radius of the circular aggregate,

$$H(0) = \sin\varphi_1\sin\theta_1\cos\theta_2 + \sin\varphi_2\cos\theta_1\sin\theta_2$$

and

$$H(\gamma) = -Re\left(\sin\theta_1\cos\theta_2\frac{ie^{i\varphi_1}}{L_{12}(\gamma)} + \cos\theta_1\sin\theta_2\frac{ie^{i\varphi_2}}{L_{12}(-\gamma)}\right)$$

The resonance interaction integrals V_a and V_b in the dipole−dipole approximation can also be determined analytically and for the orientations in Figure 5 they are equal to:

$$V_a =$$

$$d^2\frac{\sin\theta_1\sin\theta_2\left[\cos(\varphi_1 + \varphi_2) - \sin\left(\varphi_1 + \frac{\gamma - \gamma'}{2}\right)\sin\left(\varphi_1 - \frac{\gamma - \gamma'}{2}\right)\right] + \cos\theta_1\cos\theta_2}{4\pi\epsilon_0\eta^2\left(2r\sin\left(\frac{\gamma - \gamma'}{2}\right)\right)^3}$$

$$(23)$$

$$V_b =$$

$$d^2\frac{\sin\theta_1\sin\theta_2\left[\cos(\varphi_1 + \varphi_2) - \sin\left(\varphi_1 - \frac{\gamma'}{2}\right)\sin\left(\varphi_1 + \frac{\gamma'}{2}\right)\right] + \cos\theta_1\cos\theta_2}{4\pi\epsilon_0\eta^2\left(2r\sin\frac{\gamma'}{2}\right)^3}$$

$$(24)$$

where ϵ_0 is the dielectric constant and η is the refractive index of the media. Equations 21−24 explicitly demonstrate the extreme sensitivity of the CD spectra of circular aggregates on the precise orientation of the pigments.
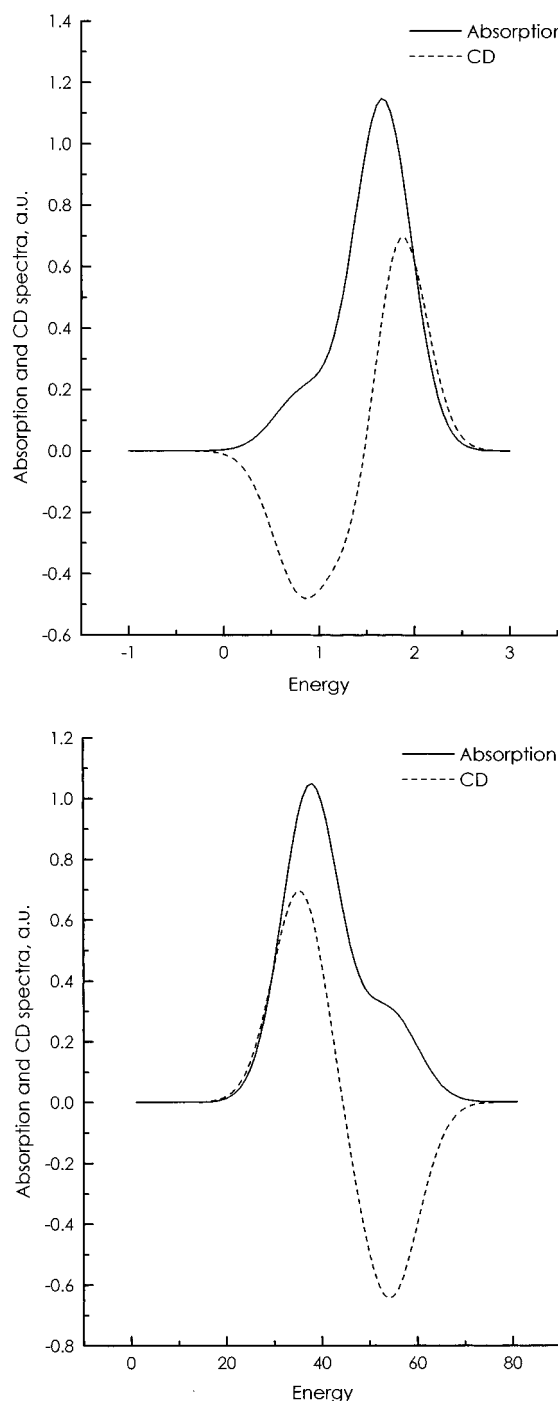

Figure 6. Absorption and CD spectra for the model aggregate shown in Figure 5. In case (a) $\phi_1 = \pi/3$, $\phi_2 = \pi/6$, $\theta_1 = \pi/4$, and $\theta_2 = \pi/7$; in case (b) $\phi_1 = \pi/5$, $\phi_2 = \pi/2$, $\theta_1 = \pi/3$, and $\theta_2 = \pi/4$. $\gamma' = 0.3\gamma$ in both cases. The site energies are $\Delta_1 = 1$ and $\Delta_2 = 1.5$, the interaction energy inside the dimer $V_b = -0.3$, homogeneous width $\delta = |V_b|$, (all energies are in au).

We will now use these results to evaluate the transition of the absorption and CD spectra of the dimer upon formation of the aggregate. Moreover, we will discuss the role of precise orientation of the individual dipole moments in the aggregate. As shown in Figure 6, changing the relative orientation of the transition dipole moments within the unit cell and between the cells strongly affects the relative position of the main absorption as well as the sign of the CD. The absorption and CD spectra shown in Figure 7 demonstrate the evolution of the spectra upon going from the dimer (i.e., when $V_a \ll V_b$ (see Figure 7a) to the full aggregate; with $V_b \sim V_a$, the latter corresponds to the situation in the LH2 structure (see Figure 7c). It can clearly be seen that the absorption spectrum is strongly influenced by the
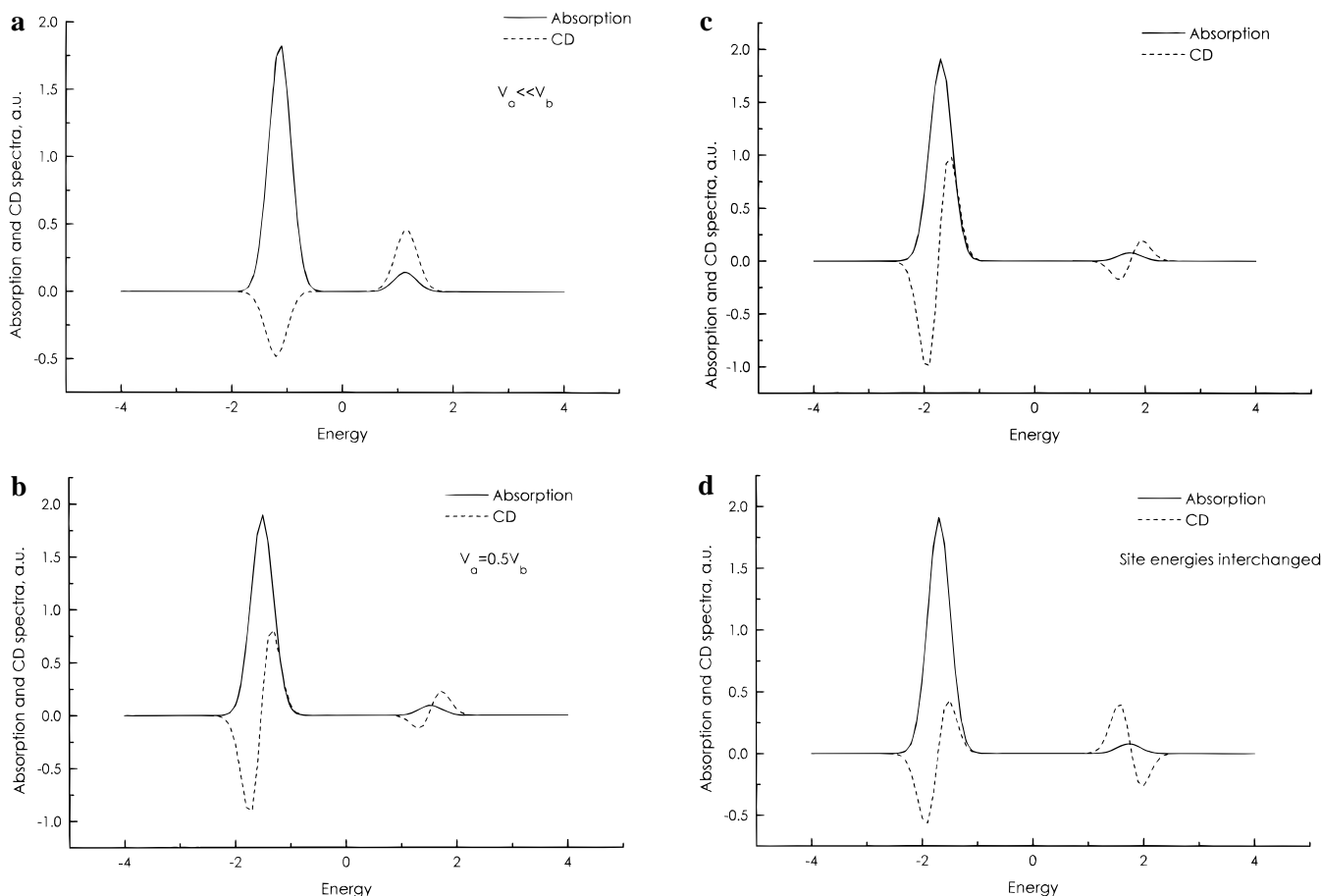
Excitons in Chains of Dimers

J. Phys. Chem. B, Vol. 101, No. 37, 1997 **7347**

Figure 7. Absorption and CD spectra for the model of the LH2 complex of *Rp. acidophila* as a function of increasing the interdimer interaction strength. The following parameters are assumed: $\phi_1 = 60°$, $\phi_2 = 68°$, $\theta_1 = 96°$, and $\theta_2 = 100°$; the energy is scaled in V_b values; thus, the interaction energy inside the dimer is assumed to be $V_b = -1.0$, homogeneous width $\delta = 0.2$, $\gamma' = 0.47\,\gamma$. (a) is the dimer (i.e., artificially assuming $V_a \ll V_b$, (b) $V_a = 0.5V_b$). (c) is the model of the LH2 (i.e., the resonance interactions are calculated according to eqs 23 and 24), the spectral heterogeneity of the molecules within the unit cell is assumed to be of the order of V_b; thus, site energies are $\Delta_1 = -0.5$ and $\Delta_2 = 0.5$ (in the units of V_b) while in the case (d) the site energies are interchanged (i.e., $\Delta_1 = 0.5$ and $\Delta_2 = -0.5$). Due to the relative energy scale used, values r, ϵ_0, and η do not influence the results.

increasing interaction between the dimers. Furthermore, relative changes in the inter- and intradimer rotational strength strongly contribute to the shape and intensity of the CD spectrum of the aggregate (see Figure 6 and Figure 7a−c). The parameters used in Figure 7 are close to those derived from the structure of LH2. The value and sign of the mismatch energy, however, is not defined. The effect due to a change in sign of the mismatch is demonstrated in Figure 7c,d.

Exciton Dynamics

To describe the exciton dynamics, the interaction of the exciton with the vibrational modes of the molecules of the aggregate, as well as that of the exciton with the vibrational modes of the surrounding medium (i.e., protein), have to be taken into account. These interactions cause the dephasing of the exciton and introduce relaxation processes, which are of paramount importance in the dynamics. They are accounted for by means of the quantum Liouville equation.[14] Since we are interested in the time evolution of the excitons only, the general Liouville equation for the whole system of excitons and vibrational modes can be averaged over the vibrational degrees of freedom. To do so, various approaches are possible. Here we will use the so-called Haken−Strobl−Reineker approach[15,16] where the vibrational subsystem is considered as δ-correlated stochastic field (white noise). Thus, for a system with two

molecules per unit cell and, consequently, with two scaling parameters the Liouville equation in the Haken-Strobl-Reineker approach reduces to:

$$i\frac{\mathrm{d}}{\mathrm{d}t}\rho_{11}(m,n) = V_a\rho_{21}(m-1,n) - V_a\rho_{12}(m,n-1) +$$
$$V_b\rho_{21}(m,n) - V_b\rho_{12}(m,n) - i\Gamma(1 - \delta_{m,n})\rho_{11}(m,n)$$

$$i\frac{\mathrm{d}}{\mathrm{d}t}\rho_{12}(m,n) = V_a\rho_{22}(m-1,n) - V_a\rho_{11}(m,n+1) +$$
$$V_b\rho_{22}(m,n) - V_b\rho_{11}(m,n) + \Delta\rho_{12}(m,n) - i\Gamma\rho_{12}(m,n)$$

$$i\frac{\mathrm{d}}{\mathrm{d}t}\rho_{21}(m,n) = V_a\rho_{11}(m+1,n) - V_a\rho_{22}(m,n-1) +$$
$$V_b\rho_{11}(m,n) - V_b\rho_{22}(m,n) - \Delta\rho_{21}(m,n) - i\Gamma\rho_{21}(m,n)$$

$$i\frac{\mathrm{d}}{\mathrm{d}t}\rho_{22}(m,n) = V_a\rho_{12}(m+1,n) - V_a\rho_{21}(m,n+1) +$$
$$V_b\rho_{12}(m,n) - V_b\rho_{21}(m,n) - i\Gamma(1 - \delta_{m,n})\rho_{22}(m,n) \quad (25)$$

where $\rho_{\alpha\beta}(m,n)$ denotes the element of the density matrix involving unit cell numbers m, n and site numbers α, β inside the unit cell. Γ is the phase relaxation rate, $\Delta = \Delta_1 - \Delta_2$.

Neglecting terms describing the phase relations between nonnearest neighbors,[15] the following equation for the diagonal

density matrix elements $\rho_\alpha(m) \equiv \rho_{\alpha\alpha}(m,m)$ can be obtained:

$$\frac{1}{\Gamma}\frac{d^2}{dt^2}\rho_1(m) + \frac{d}{dt}\rho_1(m) = w_1\rho_2(m-1) + w_2\rho_2(m) -$$
$$(w_1 + w_2)\rho_1(m)$$

$$\frac{1}{\Gamma}\frac{d^2}{dt^2}\rho_2(m) + \frac{d}{dt}\rho_2(m) = w_1\rho_1(m+1) + w_2\rho_1(m) -$$
$$(w_1 + w_2)\rho_2(m) \quad (26)$$

where $w_1 = 2V_a^2/\Gamma$ and $w_2 = 2V_b^2/\Gamma$ are excitation hopping rates. Note that now the energy mismatch Δ in the dimer has been set to zero.

Thus, eqs 26 represent a set of coupled wave-diffusion equations, which transforms to the Master equation for the hopping process in the two-component chain in the limit of large Γ. In the opposite case (i.e., for small values of Γ), eqs 25 turn into wave-like equations.

Let us now consider the cyclic molecular aggregate of relatively weakly coupled dimers (i.e., the main unit of the chain is a dimer), while the energy transfer between the dimers is nearly incoherent. In that case eqs 25 can be simplified by assuming that between dimers (i.e., $n = m \pm 1$) the phase relaxation of the off-diagonal terms $\rho_{\alpha\beta}(m,n)$ is very fast. For that case the following simplifications are valid:

$$0 \approx V_a\rho_{22}(m-1,n) - V_a\rho_{11}(m,n+1) + V_b\rho_{22}(m,n) -$$
$$V_b\rho_{11}(m,n) - i\Gamma\rho_{12}(m,n)$$

$$0 \approx V_a\rho_{11}(m+1,n) - V_a\rho_{22}(m,n-1) + V_b\rho_{11}(m,n) -$$
$$V_b\rho_{22}(m,n) - i\Gamma\rho_{12}(m,n) \quad (27)$$

All terms in eqs 27 containing V_b describe the phase relaxation between nonnearest neighbors ($n = m \pm 1$). According to our assumption of nearly incoherent energy transfer between dimers, this phase relaxation can be neglected. Thus, in analogy to eqs 26 (i.e., by neglecting these terms), the following set of equations for the second derivatives of the diagonal elements of ρ can be obtained:

$$\frac{d^2}{dt^2}\bar\rho_1(m) - \Gamma\frac{d}{dt}\bar\rho_1(m) + w_1\left(\frac{d}{dt}\bar\rho_1(m) - \frac{d}{dt}\bar\rho_2(m-1)\right) +$$
$$2V_b^2(\bar\rho_1(m) - \bar\rho_2(m)) = 0$$

$$\frac{d^2}{dt^2}\bar\rho_2(m) - \Gamma\frac{d}{dt}\bar\rho_2(m) + w_1\left(\frac{d}{dt}\bar\rho_2(m) - \frac{d}{dt}\bar\rho_1(m+1)\right) +$$
$$2V_b^2(\bar\rho_2(m) - \bar\rho_1(m)) = 0 \quad (28)$$

where $\rho(m, m) = \bar\rho(m)e^{-\Gamma t}$ (We note again that this result corresponds to the case $\Delta = 0$). The set of eqs 28 in the case of $w_1 = 0$ describes the system of uncoupled damped dimers. This set of equations is a bit more complicated than eqs 26. However, in principle, it allows us to discuss the excitation dynamics for a system, for which phase relaxation within a dimer of the unit cell is explicitly considered, while the interdimer interaction determines the nearly incoherent exciton transfer.

Discussion

In this paper we describe the spectroscopic properties and excitation dynamics of circular aggregates of dimers, with the aim to investigate the structure–function relationship of bacterial light-harvesting complexes. In the following we will first discuss the exciton spectrum of such a dimerized circular aggregate and next the exciton transfer dynamics.

Exciton Spectrum. The presence of two molecules per unit cell introduces a characteristic gap in the exciton energy spectrum, that splits the two Davydov subbands. A unit cell with the two molecules no longer equivalent can be obtained either by a difference in the resonance interactions (nondiagonal "disorder") and/or by a difference in the molecular transition energies (diagonal "disorder"). It is furthermore noteworthy that this model of a chain with two molecules per unit cell exhibits some of the essential features of a disordered aggregate. This property is illustrated by comparing the density of states as calculated according to eq 10 and presented in Figure 4 with that obtained[9] from a Monte-Carlo simulation for an aggregate with diagonal disorder.

Also, as manifested by Figures 6 and 7, the absorption and CD spectra of the circular chain of dimers are sensitive to (1) the degree of coupling between the dimers, (2) the orientation of the two molecules within the unit cell, and (3) the relative orientation of adjacent unit cells. As Figure 7 shows, for specific couplings characteristic, changes in absorption and CD spectra can be observed. For an orientation of the transition dipole moments as observed in the structure of LH2 of *Rp. acidophila*,[2,3] the absorption spectrum consists of a main transition into the state $j = \pm 1$ of the long wavelength Davydov subband and a weak transition into the same state in the blue Davydov subband. The optical transitions into states $j = 0$ of both subbands are very weak (less than 2% of the main transition) because of the preferential orientation of the transition dipole moments in the plane of the aggregate. Even assuming a small homogeneous bandwidth (of the order of 10% or less of the value of the resonance interaction between molecules within a unit cell) both transitions $j = 0$ and $j = \pm 1$ become indistinguishable in the optical spectrum; however, they are exposed in the CD spectra. Moreover, changing the sign of the relative orientation of the optical transition moments of both molecules within the unit cell does not have an effect on the absorption spectrum, but it makes a difference to the CD spectrum, which changes its sign in the blue Davydov subband. The same change of sign in the blue part of the CD spectrum occurs when interchanging the site energy values in the dimer (i.e., switching the sign of Δ (Figure 7c,d). This in principle allows one to determine the value of the energy mismatch as well as its sign. We remark, however, that this effect is sensitive to the asymmetry in θ_1 and θ_2 as well as to the amount of the mismatch between the site transition energies (see also Koolhaas et al., submitted to *J. Phys. Chem.*). For instance, for the chain with one molecule per unit cell the blue part of the exciton transition (the higher Davydov component) is absent.

Exciton Dynamics. The approach taken in this paper to describe the excitation dynamics contains many of the essential features inherent for LH2 (i.e., the excitation transfer is determined by nearly incoherent energy transfer between the main building blocks of the aggregate—dimers of coherently linked molecules (Valkunas et al., submitted to *J. Phys. Chem.*)). This approach differs from that taken by others[15,17] (see also Herman and Barvik, submitted to *J. Phys. Chem.*).

The exciton dynamics in our chain of dimers is for the case of fast relaxation of the off-diagonal terms between pigments in adjacent unit cells described by eqs 26 and 28. In general, eqs 26 and 28 are mixed hyperbolic−parabolic equations which are fairly close to the well-known *telegraphic* equations. In case friction is absent ($\Gamma = 0$) and assuming the first derivatives initially to be zero, wavelike solutions are obtained, which conserve the initial shape of the exciton distribution (nondispersive motion) and travel into opposite directions. For high
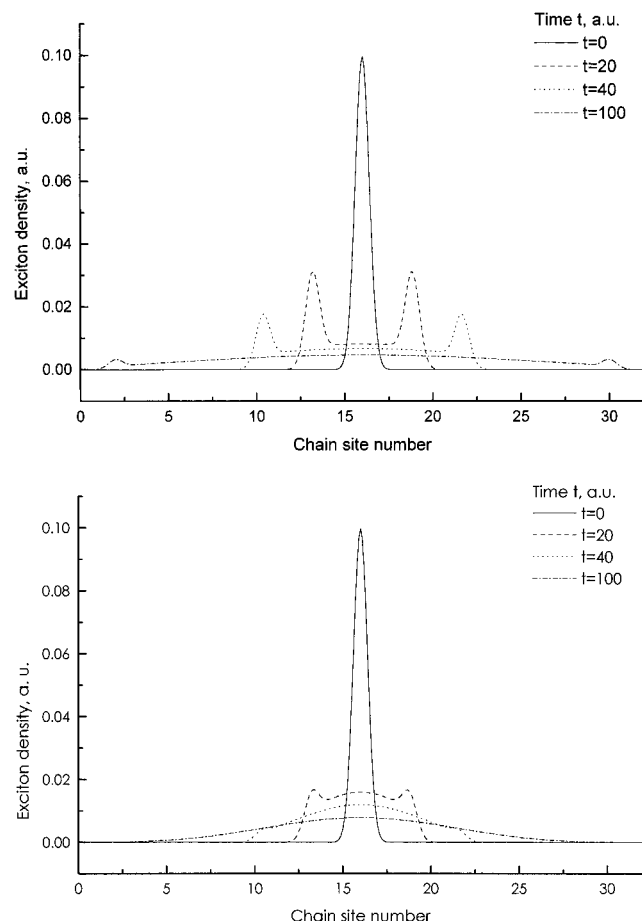
Excitons in Chains of Dimers

J. Phys. Chem. B, Vol. 101, No. 37, 1997 **7349**

Figure 8. The exciton dynamics in a dimerized chain with the number of dimers $N = 16$ assuming that at $t = 0$ the excitation is localized. The interaction energies are $V_a = V_b = -0.5$; the phase relaxation rate is in case (a) $\Gamma = 3$, and $\Gamma = 10$ in case (b) (all values in au).

values of the friction, a diffusion-like process appears, and the initial shape of exciton distribution will be lost. Such diffusion-like (incoherent exciton) movement of the excitation is widely used in the analysis of the energy transfer problem in photo-synthetic pigment−protein complexes.[1,18,19] However, the more general approach makes it possible to follow the transition from wavelike to the diffusion-like motion of the excitation, depending on the internal parameters of the system.

One of the most important questions in the discussion of the exciton dynamics on the basis of eqs 26 and 28 is the problem of initial conditions. The most fascinating behavior can be observed for localized initial conditions, which of course, is in contradiction with the implied coherent character of the exciton transport in the aggregate. It is worth to mention that these localized initial conditions could arise even in the presence of coherence in some experiments utilizing the effect of the local heating,[20,21] which produces a funnel-like relaxation, following excitation of these systems into some higher energy state. In such a case and in the absence of damping a soliton-like motion

of the excitonic density is obtained. It is interesting to note that at $\Gamma = 0$ the nearest neighbor approximation for the off-diagonal terms of the density matrix used in our approach (eqs 26) changes the exciton movement from the dispersive recon-stitution of the plane wave behavior (which exhibits t^2 like motion inherent in eqs 25) to nondispersive motion with constant velocity only. At moderate Γ values the dispersive motion of the initial exciton distribution is pronounced (see Figure 8, for instance) (i.e., the diffusion process becomes more and more dominant, erasing the solitonic features of the exciton motion).

A detailed analysis of the system of eqs 26 and 28 is rather complicated and will be presented elsewhere together with a description of the effects due to the energy mismatch within the dimer.

References and Notes

(1) Van Grondelle, R.; Dekker, J. P.; Gillbro, T.; Sundström, V. *Biochim. Biophys. Acta* **1994**, 1187.

(2) McDermott, G.; Prince, S. M.; Freer, A. A.; Hawthornthwaite-Lawless, A. M.; Papiz, M. Z.; Cogdell, R. J.; Isaacs, N. W. *Nature* **1995**, *374*, 517.

(3) Freer, A.; Prince, S.; Sauer, K.; Papiz, M.; Hawthornthwaite-Lawless, A.; MacDermott, G.; Cogdell, R. J.; Isaacs, N. W. *Structure* **1996**, *4*, 449.

(4) Kroepke, J.; Xiche, H.; Muenke, C.; Schulten, K.; Michel, H. *Structure* **1996**, *4*, 581.

(5) Karrasch, S.; Bullough, P. A.; Ghosh, R. *EMBO J.* **1995**, 14−4, 631.

(6) Novoderezhkin, V. I.; Razjivin, A. P. *Biophys. J.* **1995**, 68, 1089.

(7) Sturgis, J. N.; Robert, B. *Photochem. Photobiol*. **1996**, *50*, 5.

(8) Sauer, K.; Cogdell, R. J.; Prince, S. M.; Freer, A. A.; Isaacs, N. W.; Scheer, H. *Photochem. Photobiol.* **1996**, *64*, 3, 564.

(9) Jimenez, R.; Dikshit, S. N.; Bradforth, S. E.; Fleming, G. R. *J. Phys. Chem.* **1996**, *100*, 6825.

(10) Davydov, A. S. *Theory of Molecular Excitons*; Plenum Press: New York, 1971.

(11) Broude, V. L.; Rashba, E. I.; Sheka, E. F. *Spectroscopy of Molecular Excitons*; Springer Series in Chemical Physics 16; Springer: Berlin, 1985.

(12) Pearlstein, R. M. In *Chlorophylls*; Scheer, H., Ed.; CRC Press: Boca Raton, **1981**; p 1047.

(13) Somsen, O. J. G.; van Grondelle, R.; van Amerongen, H. *Biophys. J.* **1996**, *71*, 1934.

(14) Mukamel, S. *Principles of Nonlinear Optical Spectroscopy*; Oxford University Press: New York, 1995.

(15) Reineker, P. In *Exciton Dynamics in Molecular Crystals and Aggregates*; Hogler, G., Ed. ; Springer: Berlin, 1982.

(16) Reineker, P.; Haken, H. *Z. Phys.* **1972**, *250*, 300.

(17) Capek, V.; Barvik, I. *Phys. Rev. A* **1992**, *46*, 7431.

(18) Somsen, O. J. G.; van Mourik, F.; van Grondelle, R.; Valkunas, L. *Biophys. J.* **1994**, *67*, 484.

(19) Somsen, O. J. G.; Valkunas, L.; van Grondelle, R. *Biophys. J.* **1996**, *70*, 669.

(20) Gulbinas, V.; Valkunas, L; Gadonas, R. *Lith. J. Phys.* **1994**, *34*, 348.

(21) Gulbinas, V.; Valkunas, L.; Kuciauskas, D.; Katilius, E.; Liuolia, V.; Zhu. W.; Blankenship, R. E. *J. Phys. Chem.* **1996**, *100*, 17950.

(22) A recent publication (Wu, H.-M. Reddy, N. R. S.; Small, G. J. *J. Phys. Chem. B* **1997**, *101*, 651), which appeared after the submission of this manuscript, also considers some aspects of the absorption properties of the ring of dimers, however, using a numerical approach.